The Thermal Mass Effect of a Building Envelope in Hot Areas

K.H. Yang, Ph.D. R.L. Hwang H.T. Lin, Ph.D.

ABSTRACT

The complicated heat conduction phenomenon across building envelopes was modeled in this paper with the Thermal Response Factor method, the Conduction Transfer Function method, and the Harmonic Function method. The result was validated on the Energy Test House of a Taiwan university on a typical brick wall construction, with a time lag of five hours and significant heat wave amplitude attenuation observed.

However, the "night ventilation" design strategy was difficult to apply in the summer in this hot and humid area because of the high ambient air enthalpies. On the other had, a 30% to 40% load reduction can be obtained if properly utilized in the spring and fall at the cost of some extra ventilation power consumption.

The peak air-conditioning load reduction due to the heat wave attenuation effect is significant. High, medium, and low mass walls facing various directions were simulated with approximately 30% peak cut on west-facing walls.

INTRODUCTION

The thermal mass of building envelopes is like a heat reservoir. It absorbs heat when temperatures increase and dissipates heat when temperatures decrease.

The heat wave, traveling through the wall, thus lags behind the diurnal cycle by a phase angle, normally named the time lag, and with fluctuations "damped down" or attenuated, because of the thermal inertia encountered. However, the mass does not affect average heat flow, unless in the desert, where heat partially dissipates or radiates back to the cool night atmosphere.

In conserving energy, one design strategy is to delay much of the wall heat gain until the building is unoccupied so the air-conditioning plant is shut down and replaced with mechanical ventilation only. The other is to precool the building one or two hours before the building is occupied to relieve the overnight residual heat when the ambient temperature is low and the air-conditioning plant has better efficiencies.

On the other hand, the attenuation effect contributes to "flatten" the load pattern so that peak load is cut down significantly, which warrants a smaller air-conditioning plant.

However, in hot and humid areas, the night radiation of heat is quite unlikely since the daily temperature range is usually low. Night ventilation also might not be advantageous because of the high ambient humidity, which makes the outdoor enthalpy high. So, the energy-saving potential of thermal mass is very doubtful in this area, which necessitates a systematic study.

Dr. K.H. Yang and R.L. Hwang of the Institute of Mechanical Engineering, National Sun Yat-Sen University, Kaohsiung, Taiwan 80424, R.O.C., and Dr. H.T. Lin of the Department of Architecture, National Cheng Kung University, Tainan, Taiwan 700, R.O.C.

THEORETICAL ANALYSIS

The heat transfer phenomenon across a building envelope is dynamic in nature and getting complicated because the wall is essentially multi-layered. The conductio heat transfer is often described by the Fourier conduction equation as:

$$\partial T/\partial t = k/\rho c \cdot \partial^2 T/\partial x^2 \tag{1}$$

with the indoor boundary condition as:

$$-k_w(\partial T/\partial x)_{x=x_1} = h_i(T_{w,i} - T_i) \tag{2}$$

the interface compatibility condition of each wall layer as:

$$T_n(x,t) = T_{n+1}(x,t) \tag{3}$$

$$K_n \frac{\partial T_n(x,t)}{\partial x} = K_{n+1} \frac{\partial T_{n+1}(x,t)}{\partial x} \tag{4}$$

and the outdoor boundary condition as:

$$-k_w(\partial T/\partial t)_{x=0} = h_o(T_{o(t)} - T_{w,o}) + q_r(t) \tag{5}$$

which is a typical boundary condition of the third kind, and can be simplified by the introduction of the Sol-Air Temperature (SAT), defined as:

$$T_e = T_o + \alpha I_t/h_o - \varepsilon \Delta R/h_o \tag{6}$$

Equation 5 thus becomes:

$$q = h_o A(T_e - T_{w,o}) \tag{7}$$

or a boundary condition of the second kind.

The closed-form solution of this system of equations is extremely complicated. The semi-numerical methods, such as the Thermal Response Factor (TRF) method and the Conduction Transfer Function (CTF) method, proposed by Stephenson and Mitalas (1967, 1971) are the most popular methods.

However, since the thermal mass effect is studied here, the Harmonic Function (HF) method, using complex variable analysis, is considered the most efficient way of analyzing its time lag by the phase angle and attenuation by the amplitude of a complex variable.

The temperature distribution across the wall, after solving the above system of equations, is:

$$T(x,t) = (T_e - T_o)/(1+\varepsilon)^* x/L + T_o + \Delta T^* R_e [H_e^{-(1+i)r(1-x/L)} + e^{(1+i)r(1-x/L)}] \cdot e^{-(1+i)r+i\omega t} / 1 + H_e^{-2(1+i)r} \tag{8}$$

where

$$\varepsilon = k/hL \tag{9}$$

$$H = (\varepsilon r(1+i) - 1)/(\varepsilon r(1+i) + 1) \tag{10}$$

MODEL VALIDATION

A typical brick wall construction in Taiwan, with thermophysical properties listed in Table 1, was constructed on the Energy Test House, as shown in Figure 1. This full-scale test house, measuring 17 m by 12 m by 10 m, was equipped with two identical rooms with replaceable wall constructions in investigating their thermal performances. Each wall layer was embedded with T-type thermocouples in recording their temperature distribution.

Earlier studies by Yang and Lin (1987a,b) validated the TRF and CTR methods in evaluating the thermal performance of building envelopes. In this paper, the TRF, CTFR, and HF methods were all applied, with results compared with experimental work, as shown in Figure 2 on a typical day.

The success and close correlation of these results indicated that most temperature deviations stayed within 0.5°C, or within the measurement accuracy of a T-type thermocouple. Approximately five hours of time lag was experienced on this wall, with significant amplitude attenuation effect.

RESULTS AND DISCUSSIONS

Night Ventilation

The validation of five hours of time lag on the brick wall poses the possibility of night ventilation to flush out the residual heat penetrating into the building during unoccupied hours. However, the outdoor air enthalpies, even at night, in this area are much higher than the room air enthalpies, as shown in Figure 3. So, the enthalpy controller remained almost intact during the summer months, when cooling was most needed.

However, during spring and fall, energy savings on cooling can be obtained through optimal ventilation rates at night. Table 2 listed the result of energy savings of various thermal mass designs during April and November. The simulated normal ventilation rate was 1.5 air changes per hour (ach), which increases to 9.0 ach at night in scavenging the building. The air-conditioning system operated from 9 a.m. to 5 p.m.

The simulation was conducted utilizing the Conduction Transfer Function method in calculating the load. The result indicated that 30% to 40% load reduction can be experienced. However, the extra power consumption needed for enhanced ventilation should be taken into account.

Peak Load Reduction

The amplitude attenuation of the heat wave was quite significant, as shown in Figure 1, which warrants further study on its energy-saving potential. Different thermal masses, including high (H), medium (M), and low (L) mass envelopes, were simulated, with results shown in Figure 4.

In Figure 4, the dotted line LEMV indicates internal air-conditioning load caused by Light, Equipment, Men, and Ventilation, which stays unchanged among various cases of simulation. The conduction heat through low, medium, and high mass envelopes show significant time lag differences, with a maximum of about five hours in high-mass envelope.

As can be seen, the peak load reduction is very significant on west-facing walls with peak cuts of 530 W (from 1850 W to 1320 W of conduction heat from envelope can be experienced if high-mass envelopes were applied). However, as stated before, the average or total heat flow into the building is unchanged. So, in this aspect, the external shading device, which actually reduces the heat influx, might affect air-conditioning load reduction. This idea finally initiated another research project conducted by the author and was discussed in another paper (Yang et al. 1989).

Another interesting result about the mass affect is that the actual air-conditioner sensible and latent heat extraction (HES and HEL) of low- and high-mass walls remained fairly constant as compared to each other as shown in Figure 5. This is reasonable considering the room thermal response factors encountered in this study are fairly constant.

CONCLUSIONS

The thermal mass of walls can only delay, but not reduce, heat gains. The methodology developed in this paper, in using TRF, CTF, and HF methods, was validated successfully with experimental results conducted on the test house.

The result also indicated a five-hour time lag on a typical brick wall construction in Taiwan. However, night ventilation, in replacing mechanical refrigeration, is infeasible during the summer when cooling is most needed in this hot, humid area due to its high ambient air enthalpies. In spring and fall, load reductions up to 30% or 40% can be experienced at the cost of extra ventilation power consumption.

The attenuation of heat wave amplitude in this case is quite significant. The maximum peak load reduction can be as high as 30% on west-facing walls. Nonetheless, this effect could still be less efficient as compared with the external shading device where heat gain was partially blocked and the total heat flow rate and peak cooling load were both reduced, which warrants further systematic study.

ACKNOWLEDGMENT

The authors wish to express their appreciation to the Energy Committee of Taiwan for granting this research project.

REFERENCES

Buffington, D.E. 1975. "Heat gain by conducting through exterior walls and roofs - transmission matrix method." *ASHRAE Transactions*, Vol. 81, Part 2, pp. 96-101.

Stephenson, D.G., and Mitalas, G.P. 1967. "Cooling load calculations by thermal response factor method." *ASHRAE Transactions*, Vol. 73, Part 2, pp. 1.1-1.7.

Stephenson, D.G., and Mitalas, G.P. 1971. "Calculation of heat conduction transfer functions for multi-layered slabs." *ASHRAE Transactions*, Vol. 77, pp. 117-126.

Threlkeld, J.L. 1970. *Thermal environment engineering*. Second edition, Prentice-Hall, Inc., pp. 340-351.

Yang, K.H., and Lin, C.J. 1987a. "Calculation of dynamic heat gains before imposing load on its air-conditioning system through heat conduction transfer function." *Proceedings of the 4th National Conference of the Chinese Society of Mechanical Engineers*, December, pp. 671-679.

Yang, K.H., and Lin, C.J. 1987b. "Transfer function analysis of a conditioned building envelope on energy conservation designs." *Proceedings of the 11th National Conference on Theoretical and Applied Mechanics*, December, pp. 463-472.

Yang, K.H.; Lin, H.T.; and Chen, H.S. 1989. "The analysis of external shading effect on building energy conservation." To be presented at the ASHRAE/DOE/BTECC/CIBSE Thermal Performance of the Exterior Envelopes of Buildings IV Conference, Orlando, FL, December 4-7.

NOMENCLATURE

T = temperature
t = time
K = thermal conductivity
ρ = density
c = specific heat
x = distance
h = convective heat transfer coefficient
q_r = radiation heat
ω = harmonic frequency

Table 1

NSYSU ENERGY LAB, B-WALL TF coefficients listing

B-wall construction U=0.94375

LAYER	RHO	K	Cp	L	R,th	RC
1 tile	2400.	1.118	.2000	.0050	.0045	0.1080
2 finish	2400.	1.290	.1887	.0300	.0233	0.3166
3 brick	1650.	0.688	.2000	.1000	.1453	4.7949
4 brick	1650.	0.688	.2000	.1000	.1453	4.7949
5 air	0.	0.000	.0000	.0000	.1600	0.0000
6 wood	550.	0.155	.3110	.0040	.0258	0.0001
7 air	0.	0.000	.0000	.0000	.1600	0.0000
8 glass	2540.	0.671	.1840	.0080	.0119	0.0445
9 air	0.0	0.000	.0000	.0000	.1210	0.0000

RHO : Kg/m^3, K: Kcal/m*h*C, Cp: Kcal/Kg*C, L: m
R,th: h*m^2*C/Kcal (L/K, thermal resistance)
RC : hr (RHO*Cp*L*L/K, time constant)

NSYSU ENERGY LAB, B-WALL temp. validation (C)
BW-2 NH=12 terms of TRF= 40

HR	T	TF	TRF	Harmonic
1	24.4	24.5(+0.1)	24.5(+0.1)	24.6(+0.2)
2	24.0	24.0(-0.0)	24.0(-0.0)	23.9(-0.1)
3	23.7	23.8(+0.1)	23.8(+0.1)	23.9(+0.2)
4	23.2	23.2(+0.0)	23.2(+0.0)	23.2(+0.0)
5	22.9	23.0(+0.1)	23.0(+0.1)	23.1(+0.2)
6	22.7	22.7(+0.0)	22.7(+0.0)	22.7(+0.0)
7	23.0	23.1(+0.1)	23.1(+0.1)	23.2(+0.2)
8	23.6	23.8(+0.2)	23.8(+0.2)	23.7(+0.1)
9	24.6	24.8(+0.2)	24.8(+0.2)	24.8(+0.2)
10	26.2	26.5(+0.3)	26.5(+0.3)	26.5(+0.3)
11	27.7	27.9(+0.2)	27.9(+0.2)	27.9(+0.2)
12	29.4	30.0(+0.6)	30.0(+0.6)	29.9(+0.5)
13	32.6	34.1(+1.5)	34.1(+1.5)	34.1(+1.5)
14	38.0	39.3(+1.3)	39.3(+1.3)	39.2(+1.2)
15	40.1	41.0(+0.9)	41.0(+0.9)	41.2(+1.1)
16	35.7	35.9(+0.2)	35.9(+0.2)	35.9(+0.2)
17	33.5	33.8(+0.3)	33.8(+0.3)	33.8(+0.3)
18	31.3	31.4(+0.1)	31.4(+0.1)	31.4(+0.1)
19	29.9	30.0(+0.1)	30.0(+0.1)	30.0(+0.1)
20	28.6	28.7(+0.1)	28.7(+0.1)	28.7(+0.1)
21	27.8	27.9(+0.1)	27.9(+0.1)	27.8(+0.0)
22	27.3	27.4(+0.1)	27.4(+0.1)	27.4(+0.1)
23	25.8	26.0(+0.2)	26.0(+0.2)	26.0(+0.2)
24	25.9	26.1(+0.2)	26.1(+0.2)	26.1(+0.2)

Table 2 Cooling Load Reduction in Utilizing Night Ventilation in Kaohsiung Area

	Heavy Wall		Medium Wall		Light Wall	
	without N.V. KW needed	with N.V. "	without N.V. "	with N.V "	withoutN.V. "	with N.V. "
April	541	368	549	382	528	364
November	262	136	264	143	284	167

* Normal ventilation rate 1.5 Air change per hour
* Night ventilation rate 9.0 airchange per hour
* From May to October, night ventilation is not advantageous due to high outdoor air enthalpies.
* From December to next March, the cooling load is too small to take into account.

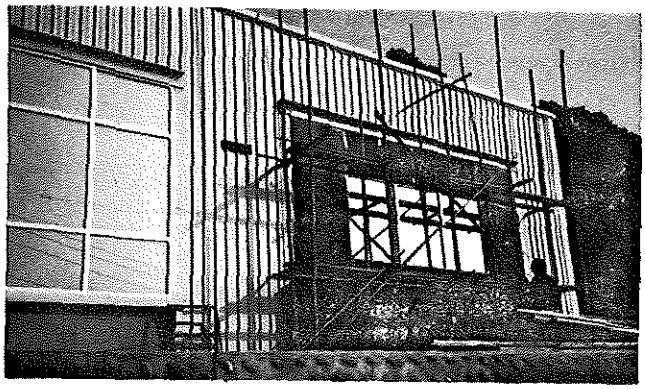

Figure 1a. *Brick wall of room B under construction*

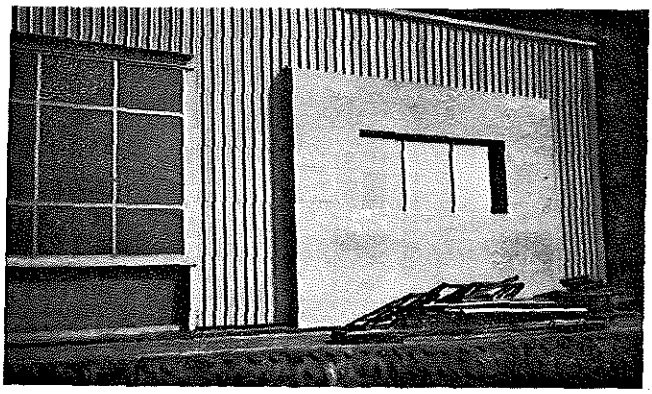

Figure 1b. *Completed room B envelope*

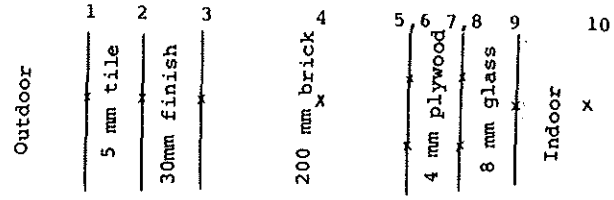

Figure 1c. *Schematic diagram of room B envelope*

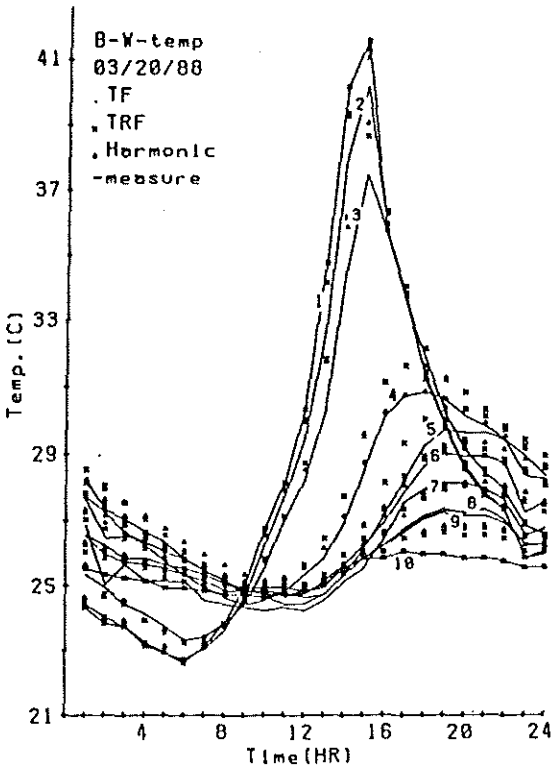

* Refer to Figure 1 for thermocouples' location

Figure 2. *Comparison of simulation and experimental results of temperature distribution across the envelope of room B*

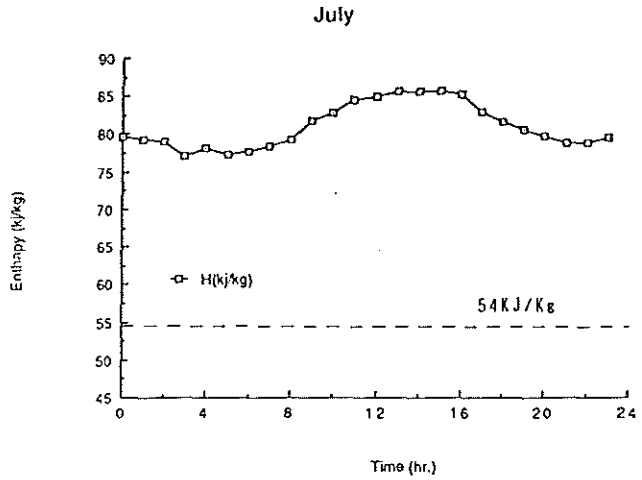

Figure 3a. *Measured outdoor air enthalpies of Kaohsiung City in July*

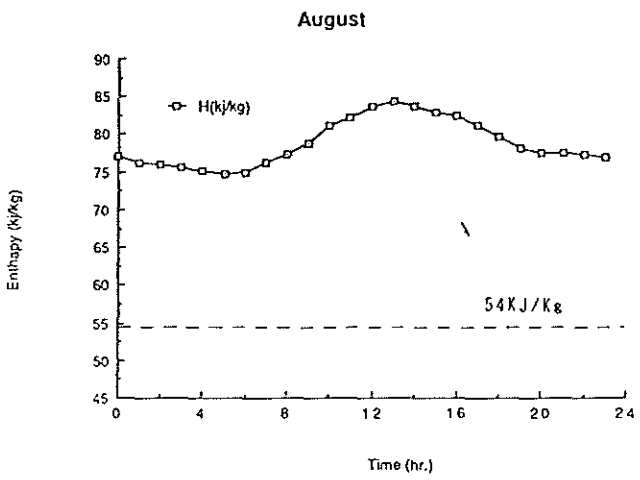

Figure 3b. *Measured outdoor air enthalpies of Kaohsiung City in August*

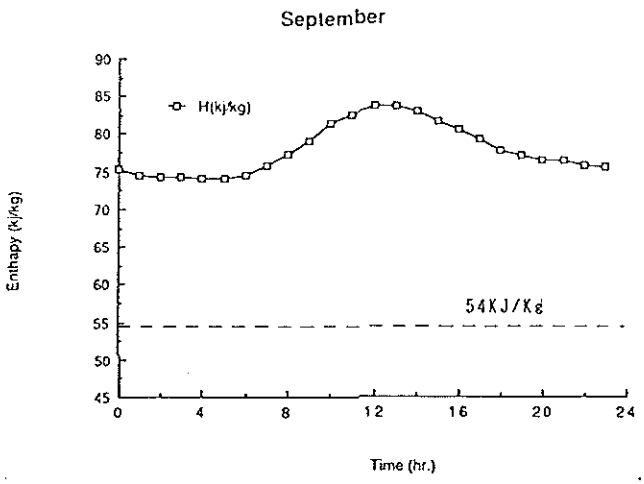

Figure 3c. Measured outdoor air enthalpies of Kaohsiung City in September

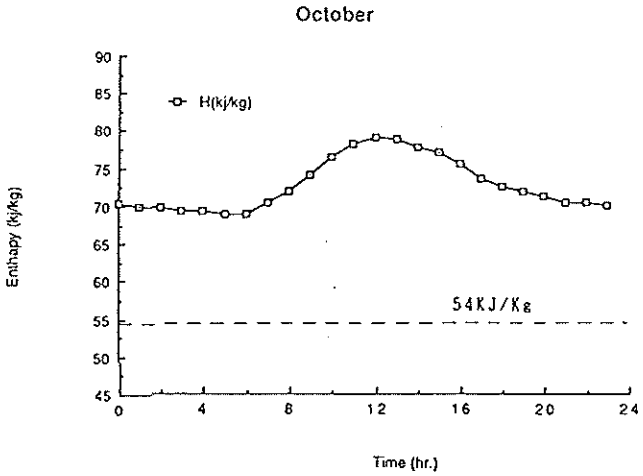

Figure 3d. Measured outdoor air enthalpies of Kaohsiung City in October

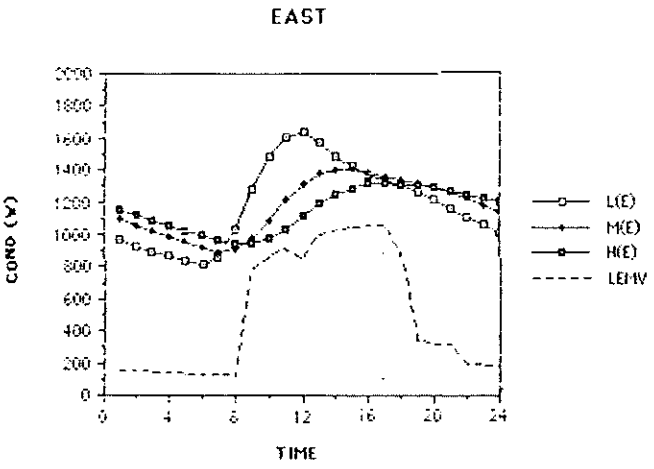

Figure 4a. Thermal mass effect on peak cooling load reduction, east-facing wall

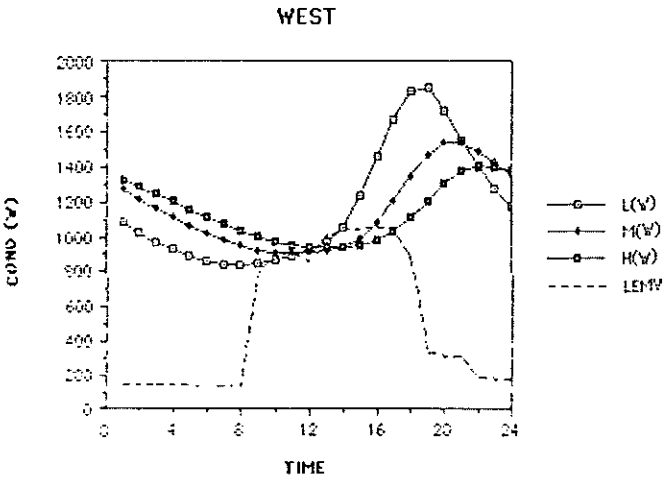

Figure 4b. Thermal mass effect on peak cooling load reduction, west-facing wall

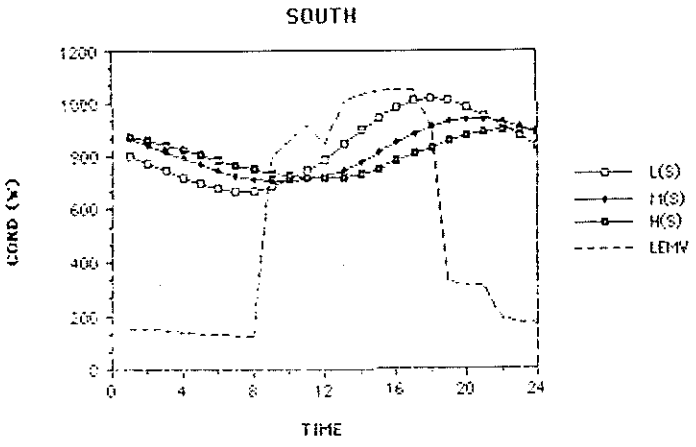

Figure 4c. Thermal mass effect on peak cooling load reduction, south-facing wall

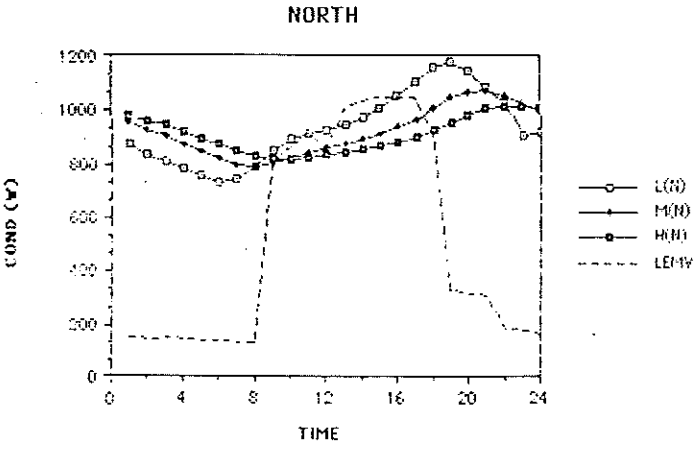

Figure 4d. Thermal mass effect on peak cooling load reduction, north-facing wall

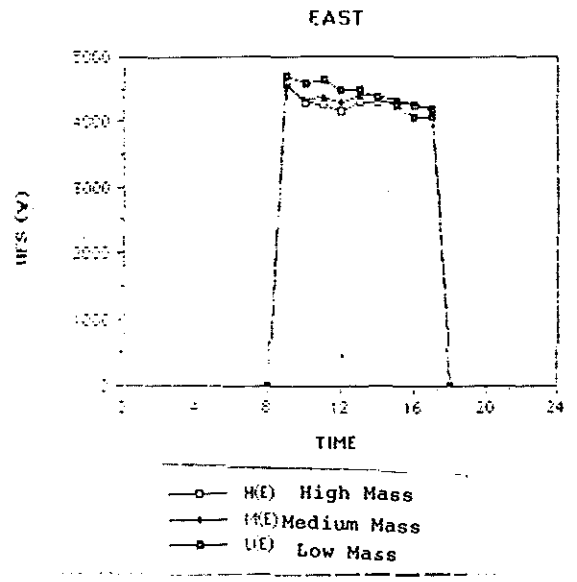

Figure 5a. Thermal mass effect on apparatus heat extraction, east-facing wall

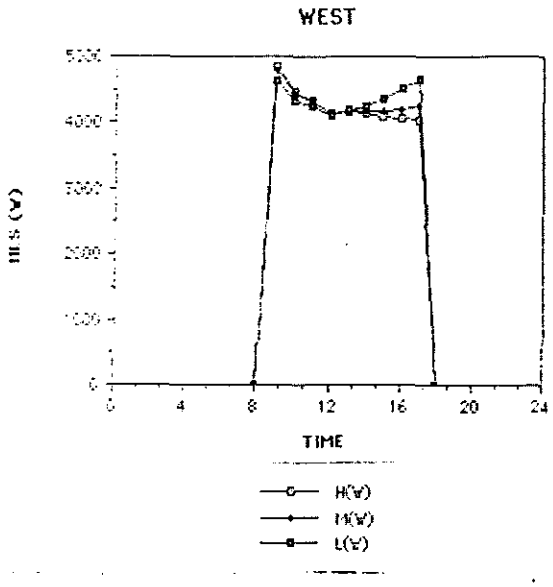

Figure 5b. Thermal mass effect on apparatus heat extraction, west-facing wall

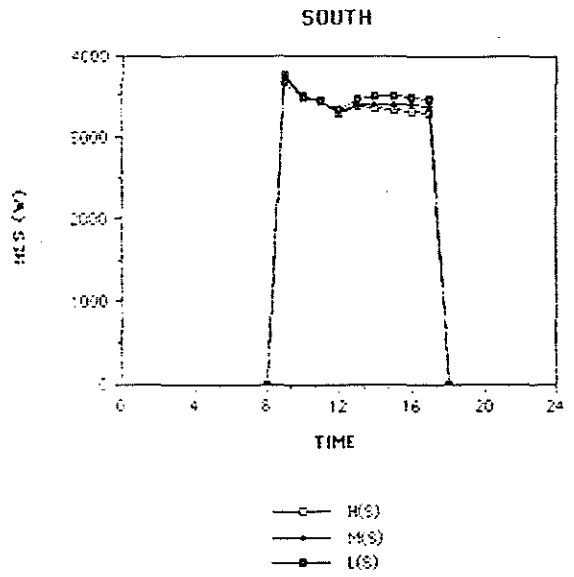

Figure 5c. Thermal mass effect on apparatus heat extraction, south-facing wall

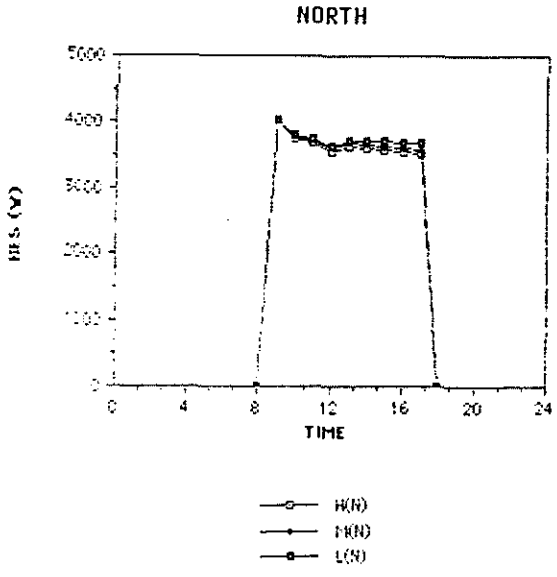

Figure 5d. Thermal mass effect on apparatus heat extraction, north-facing wall